Research Square

Preprints are preliminary reports that have not undergone peer review.
They should not be considered conclusive, used to inform clinical practice,
or referenced by the media as validated information.

SiRNA in MSCs-Derived Exosomes Silences *Ctgf* Gene for Corticospinal Axon Regeneration and Locomotor Recovery in Spinal Cord Injury Rats

Wei Huang
Affiliated Zhongshan Hospital of Dalian University
Mingjia Qu
Affiliated Zhongshan Hospital of Dalian University
Lu Li
Affiliated Zhongshan Hospital of Dalian University
Tao Liu
Affiliated Zhongshan Hospital of Dalian University
Ruimeng Duan
Affiliated Zhongshan Hospital of Dalian University
Miaoman Lin
Affiliated Zhongshan Hospital of Dalian University
Yashuai Yuan
Affiliated Zhongshan Hospital of Dalian University
Meng Zhang
Affiliated Zhongshan Hospital of Dalian University
Junxiao Gao
Affiliated Zhongshan Hospital of Dalian University
Xiaobing Yu (yuxiaobing1976@hotmail.com)
Affiliated Zhongshan Hospital of Dalian University

Research

Keywords: CTGF, spinal cord injury, exosome, small interfering RNA, RNA delivery

Posted Date: January 28th, 2020

DOI: https://doi.org/10.21203/rs.2.22022/v1

License: This work is licensed under a Creative Commons Attribution 4.0 International License.
Read Full License

Abstract

As RNA interference (RNAi) received solicitous attention by many for its promising performance in gene therapy recently, and how to obtain a choice small interfering RNA (siRNA) vector has become a moot point at this moment. Exosomes (Exo) show advantages of long survival time in vivo, high transmission efficiency and easy penetration across the blood-brain/spinal cord barrier, renowned as excellent carriers of bioactive substances. Previous studies have confirmed the detrimental effect of connective tissue growth factor (CTGF) on axonal regeneration after spinal cord injury (SCI) via stimulating the unrestricted growth of glial scars. In this study, we applied mesenchymal stem cells (MSCs)-derived Exo as the delivery of synthesized siRNA, which were extracted from rat bone marrow. We constructed exosome-siRNA (Exo-siRNA) that could specifically silence Ctgf gene in the injury sites by electroporation. During the administration, we injected Exo-siRNAs into the tail vein of SCI rats, and their distribution and accumulation in the spinal cord were visualized by in vivo fluorescence imaging. Relevant in vivo and in vitro experiments in this study showed that Exo-siRNA not only effectively inhibited the expressions of Ctgf gene and glial scar formation related proteins, such as GFAP, vimentin fibronectin and laminin, in the injured spinal cord segments, but quenched inflammation, and thwarted neuronal apoptosis and reactive astrocytes and glial scar formation. Besides, it significantly up-regulated several neurotrophic factors and anti-inflammatory factors (e.g., TGF-β1), acting as a facilitator of axon regeneration of nerve-injured motor neurons. Thus, the motor function of SCI rats were remarkably promoted. In conclusion, this study has combined the thoroughness of gene therapy and the excellent drug-loading characteristics of Exo for the precise treatment of SCI, which will shed new light on the drug-loading field of Exo.

Introduction

SCI is one of the most serious complications of spinal fracture, which mostly results in severe sensory and motor dysfunction, even paraplegia. The regeneration of damaged corticospinal axons is a critical issue that challenges doctors for years.[1] The World Health Organization has stated a rate of 40 cases of traumatic SCI per million people worldwide every year, of which up to 50% can cause varying degrees of quadriplegia.[2] MSCs with a strong potential in proliferation and differentiation has made great strides in the treatment of SCI,[3] featuring significant recovery of motor dysfunction in SCI rats. However, problems such as teratogenesis, immune rejection, pulmonary embolism, low transplantation rate and survival rate inevitably pose challenges to most researchers.[4] Recent studies have explained that the Exo secreted from MSCs may take the central role behind their potential therapeutic effect on SCI.[5] Moreover, apart from Exo's penetration across the blood-brain/spinal cord barrier depending on their small size, they also manifest a promising advantage of homing to injury sites of the central nervous system driven by inflammation.[6, 7] Their specific targeting provides the feasibility for drug delivery to the injured spinal cord segments.

Exo is nano-sized vesicles with the diameter of 30–200 nm secreted by various cells.[8] As an important means of cell-to-cell interaction, Exo can enter target cells via receptors-mediated endocytosis,

transmitting the messenger RNA (mRNA), small non-coding RNA, protein and so forth to participate in the regulation of biological information.[9–11] Numerous studies across the world have shown that intravenous injection of MSCs-derived Exo is more effective than other administrations of MSCs in repairing traumatic brain injury, stroke and other central nervous system injuries.[12] In the experiment of central nervous system injury, MSCs-derived Exo have facilitated the growth of axons of cortical neurons.[13] In stroke rats, MSCs-derived Exo have been systemically administered to promote neurovascular remodeling and restore neurological function.[14, 15] In addition, Exo derived from human umbilical cord MSCs also ameliorate the inflammatory microenvironment following SCI by down-regulating expressions of inflammatory factors, such as TNF-α, MIP-1α, IL-6 and IFN-γ.[16] The gene therapy based on stem cell-derived Exo increases medication safety, so MSCs-derived Exo as a commensurate alternative therapy can be expected for stem cell therapy.[17]

CTGF is a secretory protein with multiple regulatory functions, which plays important roles in the physiological processes of bronchial and lung formation and pathogenesis of respiratory diseases, vascular atherosclerosis and renal fibrosis.[18, 19] CTGF as a growth regulator of glial scar is essential in axon regeneration after SCI.[20] Glial scar is a chronic, physical and chemical barrier that inhibits axon regeneration of the impaired neurons in the spinal cord in mammals.[21] After SCI, CTGF is involved in initial activation of glial cells in the injury sites. Specifically, the overexpression of CTGF accelerates the proliferation of glial scars, thwarting axon migration and regeneration.[22] However, conditional deletion of CTGF significantly reverses the effect, reducing glial scar proliferation. Adenovirus- or lentiviral-mediated RNAi is the mainstream method currently used as a RNA knockout technology, which can continuously silence specific genes by introducing target siRNA into cells and continuously express it through virus infection.[23, 24, 25, 26] Despite the strong infectivity and integration of viral vectors, these exogenous viruses can easily interfere with the expressions of host genes with carcinogenic risks. Therefore, the preoccupation is to find a safer and more efficient siRNA delivery vector for clinical practice. Exo as natural vesicles secreted by autologous cells present low immune rejection and can transmit biological genetic information through blood-brain barrier. So they can be regarded as an ideal siRNA vector. Shaowei Guo et al. confirmed that loading phosphatase and tensin homolog (PTEN) siRNA with MSC exosomes significantly promoted the growth of axons and neovascularization following SCI, and significantly facilitated the rehabilitation of SCI patients.[27]

In the study of how to load siRNA into Exo, electroporation has been proved to be a good way. Faruqu Farid et al. succeeded in loading ATOT655-siRNA into human embryonic kidney (HEK)-293-derived Exo by electroporation, [28] and Aqil Farrukh et al. successfully introduced siRNA targeting v-Ki-ras2 Kirsten rat sarcoma viral oncogene homolog (KRAS) gene into milk-derived Exo by the same method, showing good loading rate and silencing efficiency.[29]

In this study, we designed and synthesized three pairs of siRNAs targeting Ctgf gene, screened out the pair with the highest silencing efficiency, effectively transfected the selected siRNA into Exo by electroporation, and explored the optimal voltage, resistance and capacitance of transfection efficiency.

In this way, we successfully constructed Exo-siRNA. In addition, our in vitro and in vivo experiments proved that Exo effectively transported siRNA to the impaired segments of spinal cord and significantly inhibited the expression of Ctgf gene. The Exo-siRNA also improved the micro-environment of injured spinal cord, inhibited inflammation and neuron apoptosis, reduced glial scars formation, facilitated axon regeneration, and promoted motor function recovery in SCI rats (Fig. 1).

Results And Discussion

Characterization of MCSs-Exo and Exo-siRNAs

As was mentioned above,[29] Exo were separated by differential centrifugation and density gradient centrifugation, and the supernatant containing affluent MSCs was extracted from the bone marrow of Sprague-Dawley (SD) rats. Characterization of Exo and the corresponding Exo-siRNAs were preliminarily compared. Transmission electron microscopy (TEM) revealed that the typical saucer-like morphology with the diameter of 30–200 nm was found in both Exo and Exo-siRNAs (Fig. 2a). Nanoparticle tracking analysis (NTA) also showed that most Exo and Exo-siRNAs were around 150 nm in diameter with little difference, indicating that the incorporation of siRNA did not affect the shape and diameter of Exo (Fig. 2b). Results of western blotting (WB) suggested that the expressions of exosome markers, CD9 and CD63, were impervious to siRNA loading (Fig. 2c).

Screening of siRNA and preliminary verification of its silencing efficiency

In the following experiment, we designed and synthesized three pairs of siRNAs (namely, siRNA-1, 2 and 3)targeting Ctgf gene, and labeled them with Cy3. The gene sequences of the three siRNAs were listed in Table 1. Their silencing efficiency was estimated. We transfected HEK293T cells with siRNA-1, 2 and 3 by Lipofectamine™ 3000 reagent (Fig. 3a), and verified by RT-PCR. The results showed that siRNA-1, 2 and 3 inhibited the expression of Ctgf gene to a certain extent, ranging from 18.85 ± 7.75% to 65.52 ± 7.52%. As a result, siRNA-2 presented stronger inhibitory effect than the other two (Fig. 3b), which was preferable to be loaded on the Exo.

Table 1
Three siRNAs designed sequences to target CTGF gene

Name	Top strand(5′→3′)	Bottom strand(5′→3′)
siRNA-1	GCUAAGUGAAGACGACAAUTT	AUUGUCGUCUUCACUUAGCCA
siRNA-2	GCCAGCUAAAGGUGAAGAUTT	AUCUUCACCUUUAGCUGGCAG
siRNA-3	CCGAUACUUCUCUCCAAAUTT	AUUUGGAGAGAAGUAUCGGTT

The MSCs-Exo presented high loading rate of siRNA with high stability

We loaded siRNA-2 into MSCs-Exo by electroporation. The EC630 (BTX, USA) electroporation system was adopted at 8 different conditions with changes in voltag, resistance and capacitance (Table 2). The loading process of the 8 groups was conducted in a pulse time of 10–15 ms. According to the reference system,28 150 μL reaction solution contained 500 nM siRNA and 7 μg Exo, and the rest was filled with electroporation buffer. Among the 8 groups, the reaction solution of Group 7 encompassed 21 μg Exo and 10 μL siRNA, and that of Group 8 21 μg Exo and 20 μL siRNA. When electroporation was accomplished, Exo were extracted from electroporation buffer and siRNA extraction, so Exo-siRNAs were obtained. Absolute quantitative Real-Time PCR results showed that Exo of the 8 groups were loaded with a certain amount of siRNAs. The loading efficiency of siRNA was the highest (Fig. 3c) in Group 2, indicating that its electroporation system was optimum. The count of siRNA nanoparticles per microgram of exosome was the highest in Group 2, reaching about 5.08×10^{11}/μg.

Table 2
Grouping according to different electroporation conditions

Conditions/Groups	1	2	3	4	5	6	7	8
Voltage (v)	400	400	400	400	400	No shocksd	400	400
Resistance(Ω)	50	50	50	50	25		150	150
Capacitor(μF)	500	200	300	400	500		500	500
Exosome volume(μl)	7	7	7	7	7	7	21	21
siRNA volume(μl)	3.75	3.75	3.75	3.75	3.75	3.75	10	20
1. SiRNA concentration: 20 μM ,Exosome concentration: 2ug/uL								
2. System: 3.75uL 20uM siRNA + 7ug exosome, the rest volume was 150uL supplemented with buffer.								

Combining results of Table 2 and Fig. 4a, it was found that the lower the capacitance, the more siRNA molecules were loaded into Exo under the same voltage and resistance conditions in Group 1 to 4. In comparison with Group 7 and 8, Group 8 presented fewer number of siRNA molecules loaded into Exo, with more siRNAs remaining in the reaction solution, than Group 7 under the same voltage, resistance and capacitance conditions. This indicated that the same electroporation condition often corresponded to an optimum concentration of siRNAs. Group 8 was the control group without electric shock, but a certain amount of siRNA could still be detected. This can be explained by the non-specific binding of siRNA to Exo. Later, we applied 5'-32P-labeled siRNA to measure siRNA loading rates in Exo. Radioactivity in the pellet and supernatant was determined by a known volume to a PEI-cellulose layer and quantitated by Packard InstantImager. The loading rate was calculated by the following formula: siRNA loading = (CPM in pellet / CPM in supernatant) × 100. Finally, the siRNA loading rates of the 8 groups were

obtained, which were in line with the corresponding RT-PCR results. Group 2 achieved the highest siRNA loading rate / electroporation efficiency, of about 33.24% (Fig. 3d). So the optimal parameters for electroporation system are as follows: voltage, 40 v; resistance, 50 Ω; capacitor, 500 μF; exosome volume, 7 μL; and siRNA volume, 3.75 μL.

In order to test the stability / anti-degradation ability of Exo-siRNA, we cultured the siRNAs delivered by blood-derived Exo with RNase A (0.01 μg/mL, simulating body fluid environment) for 45 min and naked siRNA as the control group for 45 min. The relative content of siRNA was determined by RT-PCR. As a result, the content of siRNA in exogenous siRNA was significantly higher than that of naked siRNA. After 45-min RNase A treatment, 75.1% siRNA residues remained in the exogenous siRNA group, compared with less than 50% in the naked siRNA group. This indicated that Exo as natural carriers of exogenous siRNA showed favorable encapsulation ability and effectively prevented the degradation of siRNA in body fluids. They could be renowned as ideal siRNA carriers (Fig. 3e).

In vitro study of Exo-siRNA as a treatment for SCI

Exo-siRNA effectively inhibited the expression of Ctgf gene in astrocytes and stimulated the secretion of neurotrophic factors and anti-inflammatory factors in the impaired spinal cord.

PKH67 is a green fluorescent dye that specifically binds to lipid bilayers. In this experiment, we adopted it for labeling Exo and the optimal electroporation system for effectively obtaining high amount of double-labeled Exo-siRNAs (PKH67 for Exo and Cy3 for siRNAs) for the subsequent cell and animal experiments.

Here we investigated the underlying effect of Exo-siRNAs on SCI. Rat astrocytes were treated with lipopolysaccharide (LPS) for simulating the environment of SCI, and then cultured under hypoxia (2% O_2) for 24 h. Subsequently, Exo-siRNA was co-cultured with rat astrocytes. Conventional transfection using Lipo3000 transfection reagent was used as the control group. Astrocytes of the control group were incubated with PBS (LPS/Hypoxia), while those of other three groups were administered with siRNA (LPS/Hypoxia + siRNA), Exo (LPS/Hypoxia + Exo) and Exo-siRNA (LPS/Hypoxia + Exo-siRNA). After 24-h administrations, confocal fluorescence microscopy revealed that the cells treated with Exo-siRNA were double-positive for green fluorescence (Exo) and red fluorescence (siRNAs) in Figure 4a. RT-PCR and WB uncovered that both Exo-siRNA group and the control group significantly down-regulated the expression of *Ctgf* gene, with the down-regulatory rates of 21% and 19%, respectively (Figure 4b). This indicated that Exo were competent in delivering siRNA for interfering target genes. Besides, RT-PCR results showed that Exo-siRNA facilitated secretions of neurotrophic factors (e.g., BDNF) and anti-inflammatory factors (e.g., TGF-β1) by astrocytes, which was undoubtedly of therapeutic significance of SCI (Figure 4c).

Exo-siRNA thwarted neuronal apoptosis in the impaired spinal cord segments

A previous study reported inhibitory effect of MSCs-Exo, acting as neural protectors, on neuronal apoptosis and inflammatory factors.[30] In this study, Exo-siRNA was co-cultured with LPS and dorsal root

ganglion cells (DRGs) of hypoxia-treated rats for 24 h. The DRGs in the control group were exempt from the administration of LPS/Hypoxia. The remaining four groups were SCI group (LPS/Hypoxia + PBS), siRNA treatment group (LPS/Hypoxia + siRNA), Exo treatment group (LPS/Hypoxia + Exo) and Exo-siRNA treatment group (LPS/Hypoxia + Exo-siRNA). After the 24-h administrations, cell viability was assessed by living and death staining (Figure 5a) and quantitative analysis of CCK-8 (Figure 5b). It was found that the survival rate of DRGs in SCI group was significantly reduced by less than 50%. Exo and Exo-siRNA treatment groups showed higher survival rates of DRGs than SCI group, which were close to 90.0%. There was nonsignificant difference between the two groups, indicating that the anti-apoptotic effect of Exo-siRNA mainly attributed to Exo.

Exo-siRNA propelled the balance of macrophages towards M2 in SCI environment and quenched inflammation

According to previous researches, MSCs-Exo can induce macrophage polarization and inhibit inflammation in SCI.[30-32] Here we explored the promoting effect of Exo-siRNA on macrophage polarization. NR8383 cells derived from rat alveolar macrophages were cultured with LPS/hypoxia for 24 h and then transformed into M1 state. After 48-hours incubation of siRNA, MSC-Exo and Exo-siRNA, the expressions of M1 and M2 markers were quantitated by qRT-PCR and an ELISA assay. The results showed that the expressions of M1-related pro-inflammatory cytokines, TNF-*α* and IL-6, significantly dropped in Exo or Exo-siRNA treatment groups with nonsignificant differences between the two groups (Figure 5c). Administrations of Exo and Exo-siRNA significantly boosted mRNA expressions of M2 macrophage markers, Arg-1 and CD206, without significant difference between the two groups. The expressions of anti-inflammatory factors, IL-4 and IL-10, in M2 macrophages were remarkably elevated in Exo and Exo-siRNA treatment groups (Figure 5d). However, these changes were not evident in siRNA treatment group, which indicated that siRNA had no direct regulatory effect on inflammatory factors.

In vivo study of Exo-siRNA in the treatment of SCI

Exo-siRNA passed through the blood/spinal cord barrier and accumulated at the impaired sites of SCI

We further investigated the therapeutic effect of Exo-siRNA on SCI rats. They were divided into three groups: SCI group (PBS treatment), Exo group (pure exosome treatment) and Exo-siRNA group (Exo-siRNA treatment). Exo-siRNA was administered to SCI rats by intravenous tail vein injection, and its targeting to spinal cord segments was traced by living animal fluorescence imaging system. Reference imaging required a specific wavelength range. DiR iodide (a red lipophilic fluorescent dye) was selected as the fluorescent labeling dye for Exo and Exo-siRNA. The main organs, such as heart, lung, liver, kidney and spleen, and spinal cord were harvested at 3 h, 24 h after injection and examined by fluorescence imaging system. A majority of Exo and Exo-siRNA accumulated in the liver and bilateral lungs (Figure 6a). It was found that Exo and Exo-siRNA presented relatively high fluorescence intensity in the liver based on the 3-h imaging, which was consistent with previous studies. Exo and Exo-siRNA were mainly absorbed by mononuclear phagocytes in the liver after systemic injection, and there was fluorescence in the spinal

cord, indicating chemotactic activity for Exo and Exo-siRNA in the injured spinal cord segments. The fluorescence intensity of all organs decreased dramatically 24 h after injection. Exo and Exo-siRNA were absorbed by various nerve cells in the liver and injured spinal cord.

Exo-siRNA significantly decreased the expression of Ctgf gene, inhibited the expressions of GFAP, vimentin, fibronectin and laminin, and repressed glial scar formation

To verify the silencing effect of Exo-siRNA *in vivo*, SCI rats received intravenous injection of Exo and Exo-siRNA for 5 consecutive days from the date of modeling, and the rats in sham operation group and control group were administered with the same volume of saline. At the 4th week, the damaged segments was sampled, Protein were extracted for WB analyses. Compared with SCI rats, Exo-siRNA-treated rats showed a 41.2% decrease in the corresponding protein level (Figure 6b). However, there was no evidence that Exo could also regulate CTGF. It has been proved that CTGF can down-regulate the expressions of proteins related to glial scar formation, including GFAP, vimentin, fibronectin and laminin.[24] The four proteins were determined by WB in this study. As a result, the four were down-regulated in both Exo and Exo-siRNA groups compared with SCI group . The down-regulatory rate of GFAP was 55.7%, and that of vimentin was 44.6%, fibronectin 52.2% and laminin 25.5% in Exo-siRNA group; and GFAP 25.8%, vimentin 14.5%, fibronectin 12.1% and laminin 12.9% in Exo group. Moreover, the injured spinal cord tissue of each group was collected at the 4th week. The formation of glial scar was measured by Masson staining (Figure 6c), and the area of glial scar was calculated by Image J software (V1.8.0.112). The results showed that the affected spinal cord segments by glial scar in Exo-siRNA group was 65.6%, less than the figure in SCI group. The affected area of glial scar in Exo group was 24.4%, less than that in SCI group . These results indicated that Exo repressed the formation of glial scar. However, the underlying mechanism remains unclear.[5, 33, 34]

Exo-siRNA ameliorated motor dysfunction of SCI rats

To investigate whether Exo-siRNA can restore SCI-induced motor dysfunction, Basso, Beattie and Bresnahan (BBB) locomotor scale were adopted to evaluate the motor activity of rats in each group at 1, 7, 14, 21, 28, 35, 42 and 48 days after injury. The measurement lasted 4 min. The BBB scores of all groups increased gradually with time, which indicated that rats had a certain ability of self-recovery. On the 48th day, Exo and Exo-siRNA groups exhibited significant functional recovery of locomotor activity compared with SCI group. The average score of rats in Exo-siRNA group was 15.4+1.5 points, and that in Exo group was 10.8+0.5 points. Rats in Exo-siRNA group showed better functional recovery than those in Exo group, which was consistent with and could be explained by corticospinal axon regeneration in the two groups (Figure 6d).

Exo-siRNA promoted corticospinal axon regeneration

Four weeks after modeling, the longitudinal sections of spinal cord tissues of each group were sampled. The extent of neuronal injury and glial scar formation were studied using double-labeled

immunofluorescence with neurofilament (NF-H) and glial fibrillary acidic protein (GFAP) as the corresponding markers. In SCI group, astrocytes were recruited and neurons were disintegrated compared with the control group. On the contrary, Exo and Exo-siRNA groups showed significant decreased expressions of astrocytes and increased levels of neurofilaments (Figure 7a) compared with SCI group. Due to the silencing effect of siRNA on *Ctgf* gene, Exo-siRNA group exhibited lower count of glial scars and higher count of neurofilaments than Exo group. These indicated that Exo-siRNA promoted corticospinal axon regeneration in the impaired spinal cord segments.

Materials And Methods

Preparation of MSCs and isolation of Exo

Two 2-week-old SD female rats, purchased from Animal Experimental Center of Dalian Medical University, were regularly housed. As was mentioned above,[5] bone marrow MSCs were extracted by whole bone marrow culture method and cultivated in primary culture. When the cell density reached 80%, expanded culture was carried out in complete medium with exosome-free FBS (EXO-FBS-50A, SBI, USA) for 48 h to obtain at least 200 mL cell culture supernatant.

Exo were isolated from the supernatant of MSCs by ultracentrifugation. Briefly, the supernatant was centrifuged at 500 g for 5 min and at 2000 g for 30 min at 4℃, and mixed with the equivalent volume of pre-cooled 16% PEG600 (J43968, Jinhui, Shanghai, China). The mixed solution was centrifuged at 10,000 g (E5810R , Eppendorf, Germany) for 60 min at 4℃ to remove cells and debris. In this way, the crude Exo were obtained, and were purified by centrifugation at 100,000 g for 70 min. After resuspension in PBS (LM0221A, Lianman Shanghai, China), the resulting products were purified Exo. Finally, 400 μL Exo solution (concentration at 403.1 ng/μL) was obtained and placed at - 80 °C.

Design and synthesis of Cy3-siRNA targeting *Ctgf* gene

The *Ctgf* gene sequence (sequence number: ID: 64032) in Genbank database was utilized to match the target sequence.[24] When designing siRNA, we didn't analyze the non-coding regions at 5' and 3' ends to obtain sequences (Table 1). However, target gene sequences with GC content ranging from 40% to 55% were selected as potentially preferable sequences. A program called BLAST was used to search the sequences in Genbank Expressed Sequence Label (EST) database. The selected sequences were compared on the basis of the corresponding genome library to exclude homologous sequences from other coding ones for determining their specific sequences thereby. To provide the sequence of target gene fragment for further synthesis by Shanghai Meixuan Biological Company (China), three pairs of target gene siRNAs corresponding to different regions were designed and labeled by fluorescent dye Cy3.

Preliminarily analysis for the inhibition efficiency of RNAi

The target gene-*Ctgf* fusion transcript reporter system constructed above aimed to explore the inhibition efficiency of the three siRNAs.[35] HEK293T cells (Cytobank of Saibao, Shanghai, China) were seeded in 6-well plates (6×10^5 cells per well) and grown overnight at 37°C with 5% CO_2. SiRNA-1, 2 and 3 of 1 μg were cotransfected into HEK293T cells using Lipofectamine™ 3000 (Thermo, Shanghai, China). The HEK293T cells without transfection were used as a control. After cotransfection, the expression of *Ctgf* gene in HEK293T cells was detected at 72 h by fluorescence microscope (IX71; Olympus, Tokyo, Japan) to preliminarily analyze the inhibition efficiency of RNAi. At the same time, the total RNA of transfected cells was extracted and *Ctgf*-related mRNAs were analyzed by qRT-PCR (All sequences of primer pairs used were listed in the section of qRT-PCR).

Exosome staining

According to one research,[36] the stored Exo were taken out from the fridge and melted. After complete melting, 200 mL Diluent C (B8003S, Bomez, USA) was added to an EP tube, labeled as A tube, and carefully mixed. Then 300 μL Diluent C and 4 μL PKH67 dye (BB-441112, BestBio, Shanghai, China) were added to another EP tube (1.5 mL), the B tube, and the dye solution was fully mixed. The solution of A and B tubes was mixed and incubated at room temperature for 5 min. The reaction between Exo and dye solution was terminated for 1 min by adding 600 μL 1% bovine serum albumin (BSA). Then the volume of the mixture was added to 20 mL and centrifuged for 60 min at 120,000 g. When the supernatant was discarded, the remaining part was suspended by PBS. The sedimentation was PKH67-Exo.

The loading efficiency of siRNA

As was mentioned earlier,[28] we intended to load siRNA into the PKH67-Exo by electroporation using the EC630 electroporation system (BTX, USA). PKH67-Exo was diluted to 0.5 mg/mL in siRNA electroporation buffer (BTX, USA). Target gene Cy3-siRNA and fluorescently-labeled control siRNA were added at a final concentration of 100 nM. The mixtures were transferred into ice cold 0.4-cm cuvettes and electroporated under 8 different conditions, involving changes in voltag, resistance and capacitance (Table 2) with a pulse time of 10-15 ms. Electrical perforation was performed once in each condition. Samples were kept on ice for at least 15 min before and after an electroporation pulse. The post-electroporation samples were centrifuged at 8,000 g for 5 min for pellet aggregates. Cy3-siRNA without Exo was also electroporated to serve as control. Finally, after exosome extraction from electroporation buffer and siRNA extracts, reverse transcription and qPCR detection were performed, and double fluorescent labeled Exo-siRNA was obtained.

Quantitative determination of siRNA-loading capacity in Exo

Loading capacity: To determine siRNA-loading capacity, the 32P-labeled siRNA was adopted as a tracer using the optimal silencing efficiency which had been screened out in the previous process. The reaction

conditions for electroporation were described above. After terminating the reaction, Exo were collected by precipitating with ExoQuick-TC reagent (System Biosciences, Palo Alto, CA, USA) on ice for 1 h followed by centrifugation at 13,000X g for 5 min and the pellet was resuspended in PBS. The supernatant was collected separately. Radioactivity in the pellet and supernatant was determined by a known volume to a PEI-cellulose layer and quantitated by Packard InstantImager. The siRNA-loading capacity was calculated by the aforesaid formula.

siRNA y stability siRNA: Exo loaded with 5'-32P-labeled siRNA were incubated with various concentrations of RNase A (0.01 μg/mL, Sigma, USA). After incubation at 37 °C for 45 min, naked siRNA was used as control. Quantitative analysis of undegraded siRNA was performed by RT-PCR.

Co-culture of Exo-siRNA with astrocytes, DRGs and macrophages in SCI environment

Co-culture with astrocytes

Rat astrocytes (ATCC, Chinese Academy of Sciences cell bank) were inoculated on 12-well plate, with 5 × 10^4 cell/well. The 2 mL DMEM medium (Thermo, 11965-092) encompassed 10% fetal bovine serum (Gibco, 10099-141), 100 μg/mL streptomycin (Gibco) and 100 U/mL penicillin (Gibco). When astrocytes fused to about 90%, the SCI environment was simulated by 100 μL LPS (10 μg/mL, Jinhui, China) and hypoxia (2% O_2) for 24 hours. Cell grouping (n = 3): SCI group was treated with 50 μL PBS; siRNA group was incubated by 2 μL lipo3000 (Thermo, L3000015) and 50 nM Cy3-siRNA, as negative control (NC); Exo group was added with 50 μL Exo; and Exo-siRNA group contained 50 μL Exo-siRNA. RNAs were extracted 48 h after incubation for further quantitative RT-PCR analysis. Proteins were also extracted for WB.

Co-culture with DRGs

Rat spinal DRGs (ATCC, Chinese Academy of Sciences cell bank) were sampled. Cell culture, seedboard, grouping and administration were the same as those of the astrocytes which were mentioned above. It was noted that cells of the control group were not treated with LPS/hypoxia. After the 24-h administration, DRG neurons were washed with PBS twice and stained in situ. Each 12-well plate was rearranged with 200 μL Calcein-AM/PI double staining reagent (Saibaikang, HR0444, China) and the neurons were incubated at 37°C for 25 min. Cells of all groups were observed by fluorescence microscopy (Olympus, IX70, Japan) with the 490 nm excitation wavelength. Yellow/green fluorescence indicated living cells, and red fluorescence marked dead cells. Cell viability was detected by CCK-8. Cell suspension was collected and inoculated into a 96-well plate (100 μL per well). Subsequently, 10 μL of CCK-8 solution (Abbkine, KTC011001) was added to each well and incubated for 2.5 h. The absorbance (OD) at 450 nm was measured by an enzyme immunoassay microplate reader.

Co-culture with macrophages

Rats NR8383 macrophages (ATCC, Chinese Academy of Sciences cell bank) were obtained. Cell culture, seed plate, grouping and administration were the same as those of astrocytes. After 48-h treatment, RNAs were extracted for RT-PCR analysis and an ELISA assay was adopted to detect expressions of various inflammatory factors using the following kits: rat IL-1β ELISA kit (Cusabio, China), rat TNF-α ELISA kit (Cusabio, China), rat IL-6 ELISA kit (Cusabio, China), rat IL-4 ELISA kit (Cusabio, China), rat IL-10 ELISA kit (Cusabio, China) and rat VEGF ELISA kit (Cusabio, China). Cell supernatant was collected and centrifuged for 20 min at 1,000 g. The OD at 450 nm was measured by an ELISA reader.

Establishment, grouping and tail-vein administration of SCI rat models

The animal experiments in this study were reviewed and approved by the ethics committee of Affiliated Zhongshan Hospital of Dalian University. One hundred SD female rats (200-250 g, 10 weeks old) were randomly divided into 5 groups: SCI group (PBS treatment), Sham group (PBS treatment), siRNA group (siRNA treatment), Exo group (pure exosome treatment) and Exo-siRNA group (Exo-siRNA treatment) with 20 rats in each group. Rats were anaesthetized with sodium pentobarbital (Sigma, St. Louis Mo, USA). An incision of 2cm was made at T10 level to expose skeletal muscles of spinal cord in sterile environment. Lateral vertebral muscles were separated from the bone margin of articular process. Spinous processes and laminae were removed and T10 was exposed as an impact zone. Except for the Sham group, receiving a sham operation, rats of the rest groups were hit on the T10 segment using a spinal cord impactor (PSI, IH-0400, USA), with metal rod weight of 30 g and height of 50 mm. After that, bilateral hind limbs were involuntarily twitching and tails swinging in all animals, indicating that the injury corresponded to the standard of a SCI model. After the suture of muscle layer and skin, rats were allowed to recover in heat preservation chambers. Postoperative nursing of SCI rats mainly encompassed daily artificial bladder emptying and restoration of bladder reflex activity. Tail-vein administration was performed every 24 h for 5 consecutive days, and the dosage was as follows: SCI group and Sham group were administered with 150 μL PBS; while siRNA group with 150 μL siRNA (0.2 nmol), Exo group with 150 μL exosome solution and Exo-siRNA group with 150 μL Exo-siRNA solution.

Quantitative qRT-PCR

A RNA extraction kit (Solarbio, China) was used to extract total RNA from various cells and spinal cord tissues. SiRNAs from Exo or cells were extracted by a miRNA extraction kit (Solarbio, China). Target mRNA or siRNA was used as template, and the total RNA reverse-transcribed into cDNA using a reverse transcription kit (Solarbio, China). The volume of the whole reaction system was 15 μL, which was maintained at 16℃ for 30 min, 42℃ for 30 min and 85 ℃ for 5 min. A universal PCR kit (Solarbio China) was used for PCR amplification using cDNA as template. Quantitative qRT-PCR was performed under the following amplification conditions: 95 ℃ for 20 s, followed by 40 cycles of denaturation at 95

℃ for 3 s with extension at 60 ℃ for 30 s. The reaction repeated three times. *Gapdh* was adopted as an internal reference gene for relative quantification by the $2^{-\Delta\Delta Ct}$ method.

Western blotting

Total protein of Exo, cells or spinal cord tissues was extracted using RIPA buffer (Jinhui, Shanghai, China) and protein concentration was evaluated with a BCA assay (Jinhui, Shanghai, China) according to the manufacturer's protocol. Proteins (50 μg per lane) were separated by 10% SDS-PAGE and transferred to polyvinylidene difluoride membranes. The membranes were blocked using 5% non-fat dry milk in TBST at 37˚C for 1 h and incubated with primary antibodies at 4˚C overnight. All primary antibodies included CD9, CD63, GAPDH, CTGF, GFAP, vimentin, fibronectin, laminin, HGF, VEGF, BDNF, TGF-β1, Bcl-2 and Caspase-3 (Abcam, UK). Subsequent to washing with PBST for 20 min, membranes were incubated with anti-rabbit horseradish peroxidase-conjugated secondary antibody (Abcam, UK) at 37˚C for 1 h. Protein blanks were visualized with an enhanced chemiluminescence kit (Promo Cell, Germany).

Immunofluorescence Analysis

Rat spinal cords were sectioned on a cryostat set at 20-μm intervals. Sections were permeabilized in 0.5% Tween solution, blocked with 5% bovine serum, and then incubated with rabbit GFAP antibody (1:100, Abcam, UK) and mouse neurofilament NF-H antibody (1:1000, Biorbyt, UK) at 4°C overnight. After that, sections were incubated with goat anti-rabbit IgG (H+L) secondary antibody (1:300, Invitrogen), and DAPI (1:1000) for 1 h, mounted with coverslips, and confocal fluorescence microscope (Leica Microsystems DM i8) was performed to obtain images.

Masson staining

After 28 days, the spinal cords of rats were harvested and sectioned (2 mm) in cross section. After dewaxing, the samples were washed with distilled water three times. Then they were stained with nuclear dye for 2 min, destained with 1% hydrochloric acid alcohol (75% alcohol : concentrated hydrochloric acid = 99:1) for 1 s, blue in running tap prior to cytoplasmatic staining for 30-60 s. Finally, color separation solution for 1-3 min and the sections were transferred to aniline blue solution and stained for 5 min. The slides were dehydrated and the tissue was mounted with a coverslip. The accomplished slides of spinal cords were observed under a confocal microscope (Leica Microsystems SD AF).

BBB locomotor scale

Rat locomotor recovery was estimated by the BBB locomotor rating scale, ranging from 0 point (no motor activity) to 21 points (normal locomotion). Two independent investigators blinded to the treatment

assessed the locomotor activity with corresponding scores at 1, 7, 14, 21, 28, 35, 42 and 48 days after modeling.

Statistical analysis

Statistical analyses were performed using MATLAB/GraphPad Prism software. Student *t* test was utilized for two group comparison. One-way ANOVA was adopted to compare the differences between groups while multiple comparisons were performed by Tukey's post hoc test (Graphpad Prism 8.0). *P* values of <0.05 indicated statistical significance. Significance levels were represented as $*p < 0.05$ and $**p < 0.01$.

Conclusion

This study demonstrates that Exo-siRNA presents high targeting ability in vivo and its feasibility for repairing the injured spinal cord. Exo act not only as efficient carriers for biologically active molecules, but prominent facilitators for resisting neuronal apoptosis, stimulating the secretion of neuroprotective factors and anti-inflammatory factors and ameliorating microenvironment of impaired spinal cord. These effects mainly attribute to the integrated function of various RNAs, proteins and other messenger molecules contained in Exo, which requires further precise analysis and clarification. However, exosome, a non-invasive, rapid and cell-free deliverer with low specificity, shows broad prospects and will inspire more effective methods for the treatment of SCI.

Declarations

Author information

Corresponding Author *E-mail: yuxiaobing1976@hotmail.com

Availability of data and materials

All data generated or analyzed during this study are included in this published article.

Authors' contributions

Conceptualization: Wei Huang, Mingjia Qu，Lu Li.

Investigation: Ruimeng Duan, Depeng Shang.Lu Li

Methodology: Meng Zhang,Yashuai Yuan.

Resources: Xiaobing Yu, Mingjia Qu.

Supervision: Xiaobing Yu ,Wei Huang,Lu Li.

Writing – original draft: Wei Huang, Mingjia Qu,Xiaobing Yu.

Writing – review & editing: Wei Huang, Xiaobing Yu.

Funding

There is no fund support here.

Ethics approval and consent to participate

This work was supported by Affiliated Zhongshan Hospital of Dalian University according to Laboratory Animal Welfare and Ethical review.

Consent for publication

All the authors have approved the manuscript and agree with submission to

your esteemed journal.

Competing interests

The authors declare that they have no competing interests.

References

1. FE, P.; neurology, N. H. J. E., Serotonergic mechanisms in spinal cord injury. **2019,** *318* (undefined), 174-191.
2. FA, R.; JE, G.; JD, R.; AJ, H.; J, L.; medicine, D. J. J. A. o. p.; rehabilitation, Medical rehabilitation after natural disasters: why, when, and how? **2012,** *93* (10), 1875-81.
3. P, A.; GJ, D.; BJ, H.; JR, P.; neuroscience, T. W. J. N., Cell transplantation therapy for spinal cord injury. **2017,** *20* (5), 637-647.
4. H, S.-P.; R, R.; J, M.; L, R.; CR, C.; S, H.; N, A.; sciences, A. M. J. L., Intra-bladder wall transplantation of bone marrow mesenchymal stem cells improved urinary bladder dysfunction following spinal cord injury. **2019,** *221* (undefined), 20-28.
5. JH, H.; XM, Y.; Y, X.; CC, X.; X, L.; FB, Y.; Y, C.; neurotrauma, L. F. J. J. o., Systemic Administration of Exosomes Released from Mesenchymal Stromal Cells Attenuates Apoptosis, Inflammation, and Promotes Angiogenesis after Spinal Cord Injury in Rats. **2017,** *34* (24), 3388-3396.
6. N, P.; O, B.; R, S.; S, B.; A, A.; T, S.; U, A.; R, P.; letters, O. D. J. N., Golden Exosomes Selectively Target Brain Pathologies in Neurodegenerative and Neurodevelopmental Disorders. **2019,** *19* (6), 3422-3431.
7. G, M.; CV, C.; EJ, H.; JR, P.; LI, Z.; N, M.; TE, P.; DE, I.; CC, D.; nano, M. M. J. A., Tumor-Derived Extracellular Vesicles Breach the Intact Blood-Brain Barrier Transcytosis. **2019,** *undefined*

(undefined), undefined.

8. DM, P.; biochemistry, G. S. J. A. r. o., Exosomes. **2019,** *88* (undefined), 487-514.
9. M, T.; Cell, T. C. J., Communication by Extracellular Vesicles: Where We Are and Where We Need to Go. **2016,** *164* (6), 1226-1232.
10. S, P.; Cell, S. J. J., Explicating Exosomes: Reclassifying the Rising Stars of Intercellular Communication. **2019,** *177* (2), 225-227.
11. DK, J.; AM, F.; JL, F.; JN, H.; Q, Z.; LJ, Z.; DC, L.; J, P.; Q, L.; R, E.; WH, F.; JG, P.; LH, R.; DT, B.; Cell, C. R. J., Reassessment of Exosome Composition. **2019,** *177* (2), 428-445.e18.
12. JK, W.; neurology, S. R. J. C. o. i., Traumatic brain injury: recent advances in plasticity and regeneration. **2015,** *28* (6), 565-73.
13. Y, Y.; Y, Y.; X, S.; J, H.; W, B.; neuroscience, H. X. J. F. i. c., MSCs-Derived Exosomes and Neuroinflammation, Neurogenesis and Therapy of Traumatic Brain Injury. **2017,** *11* (undefined), 55.
14. Y, Z.; M, C.; Y, M.; M, K.; H, X.; A, M.; neurosurgery, X. Y. J. J. o., Effect of exosomes derived from multipluripotent mesenchymal stromal cells on functional recovery and neurovascular plasticity in rats after traumatic brain injury. **2015,** *122* (4), 856-67.
15. ZG, Z.; B, B.; Neurology, C. M. J. N. r., Exosomes - beyond stem cells for restorative therapy in stroke and neurological injury. **2019,** *15* (4), 193-203.
16. Sun, G.; Li, G.; Li, D.; Huang, W.; Zhang, R.; Zhang, H.; Duan, Y.; Wang, B. J. M. S.; C, E., hucMSC derived exosomes promote functional recovery in spinal cord injury mice via attenuating inflammation. **2018,** *89*.
17. M, M.; K, R.; transplantation, S. E. J. B. m., Mesenchymal stem cell-derived exosomes for clinical use. **2019,** *54* (null), 789-792.
18. X, W.; H, C.; pharmacology, W. S. J. E. j. o., CTGF: A potential therapeutic target for Bronchopulmonary dysplasia. **2019,** *860* (undefined), 172588.
19. Q, Y.; medicine, L. H. J. A. i. e.; biology, Connective Tissue Growth Factor and Renal Fibrosis. **2019,** *1165* (undefined), 365-380.
20. S, O.; H, T.; SU, K.; Cellular, S. J. J.; neurobiology, m., Gene expression profiling of human neural progenitor cells following the serum-induced astrocyte differentiation. **2009,** *29* (3), 423-38.
21. AP, T.; PM, W.; reviews, S. J. J. P., The Biology of Regeneration Failure and Success After Spinal Cord Injury. **2018,** *98* (2), 881-917.
22. MH, M.; C, P.; AL, D.; T, E.; DY, S.; Science, P. K. J., Injury-induced ctgfa directs glial bridging and spinal cord regeneration in zebrafish. **2016,** *354* (6312), 630-634.
23. Lu, L.; Wang, Y.; Zhang, F.; Chen, M.; Lin, B.; Duan, X.; Cao, M.; Zheng, C.; Mao, J.; Shuai, X. J. A. F. M., MRI-Visible siRNA Nanomedicine Directing Neuronal Differentiation of Neural Stem Cells in Stroke.
24. Y, W.; QJ, K.; JC, S.; Y, Y.; HB, W.; Q, Z.; Society, S. J. J. T. s. j. o. j. o. t. N. A. S., Lentivirus-mediated silencing of the CTGF gene suppresses the formation of glial scar tissue in a rat model of spinal cord

injury. **2018,** *18* (1), 164-172.

25. Danilov, C. A.; Steward, O. J. E. N., Conditional genetic deletion of PTEN after a spinal cord injury enhances regenerative growth of CST axons and motor function recovery in mice. **2015,** *266*, 147-160.
26. EA, G.; MM, B.; neurology, S. O. J. E., Long-term consequences of conditional genetic deletion of PTEN in the sensorimotor cortex of neonatal mice. **2016,** *279* (undefined), 27-39.
27. S, G.; N, P.; O, B.; S, B.-S.; A, S.; I, M.; R, P.; D, O.; nano, L. S. J. A., Intranasal Delivery of Mesenchymal Stem Cell Derived Exosomes Loaded with Phosphatase and Tensin Homolog siRNA Repairs Complete Spinal Cord Injury. **2019,** *undefined* (undefined), undefined.
28. FN, F.; L, X.; JoVE, A.-J. K. J. J. o. v. e., Preparation of Exosomes for siRNA Delivery to Cancer Cells. **2018,** *undefined* (142), undefined.
29. F, A.; R, M.; J, J.; AK, A.; AH, K.; SA, W.; letters, G. R. J. C., Milk exosomes - Natural nanoparticles for siRNA delivery. **2019,** *449* (undefined), 186-195.
30. HY, K.; H, K.; MJ, J.; J, K.; JK, Y.; JR, L.; M, K.; YW, C.; SY, S.; SP, K.; T, H.; IB, H.; letters, K. B. J. N., Therapeutic Efficacy-Potentiated and Diseased Organ-Targeting Nanovesicles Derived from Mesenchymal Stem Cells for Spinal Cord Injury Treatment. **2018,** *18* (8), 4965-4975.
31. X, W.; K, C.; X, S.; Y, C.; Z, D.; L, S.; L, G.; P, B.; D, S.; J, F.; X, H.; W, Y.; Glia, R. Y. J., Macrophages in spinal cord injury: phenotypic and functional change from exposure to myelin debris. **2015,** *63* (4), 635-51.
32. R, S.; O, M.; G, Y.; N, R.; A, L.; J, R.; KW, K.; E, K.; V, K.; P, B.; SA, L.; S, J.; Immunity, S. M. J., Recruitment of beneficial M2 macrophages to injured spinal cord is orchestrated by remote brain choroid plexus. **2013,** *38* (3), 555-69.
33. W, L.; Y, W.; F, G.; Y, R.; Y, L.; P, T.; Z, Z.; Z, Z.; T, X.; T, J.; S, Y.; G, Y.; J, C.; J, F.; neurotrauma, C. W. J. J. o., Exosomes Derived from Bone Mesenchymal Stem Cells Repair Traumatic Spinal Cord Injury by Suppressing the Activation of A1 Neurotoxic Reactive Astrocytes. **2019,** *36* (3), 469-484.
34. MB, G.; T, M.; E, C.; CJ, H.; J, G.; C, H.; D, T.; M, R.; M, A.; P, D.; TP, C.; Neuroscience, C. J. J. T. J. o. n. t. o. j. o. t. S. f., Neuronal RARβ Signaling Modulates PTEN Activity Directly in Neurons and via Exosome Transfer in Astrocytes to Prevent Glial Scar Formation and Induce Spinal Cord Regeneration. **2015,** *35* (47), 15731-45.
35. H, Z.; X, L.; Q, W.; F, L.; Z, F.; C, L.; Z, L.; T, C.; T, W.; L, L.; G, N.; X, K.; medicine, F. S. J. R., shRNA against PTEN promotes neurite outgrowth of cortical neurons and functional recovery in spinal cord contusion rats. **2015,** *10* (4), 411-29.
36. B, X.; Y, Z.; XF, D.; J, L.; HX, Z.; JW, B.; Y, Y.; H, H.; research, D. J. J. C., Neurons secrete miR-132-containing exosomes to regulate brain vascular integrity. **2017,** *27* (7), 882-897.

Figures

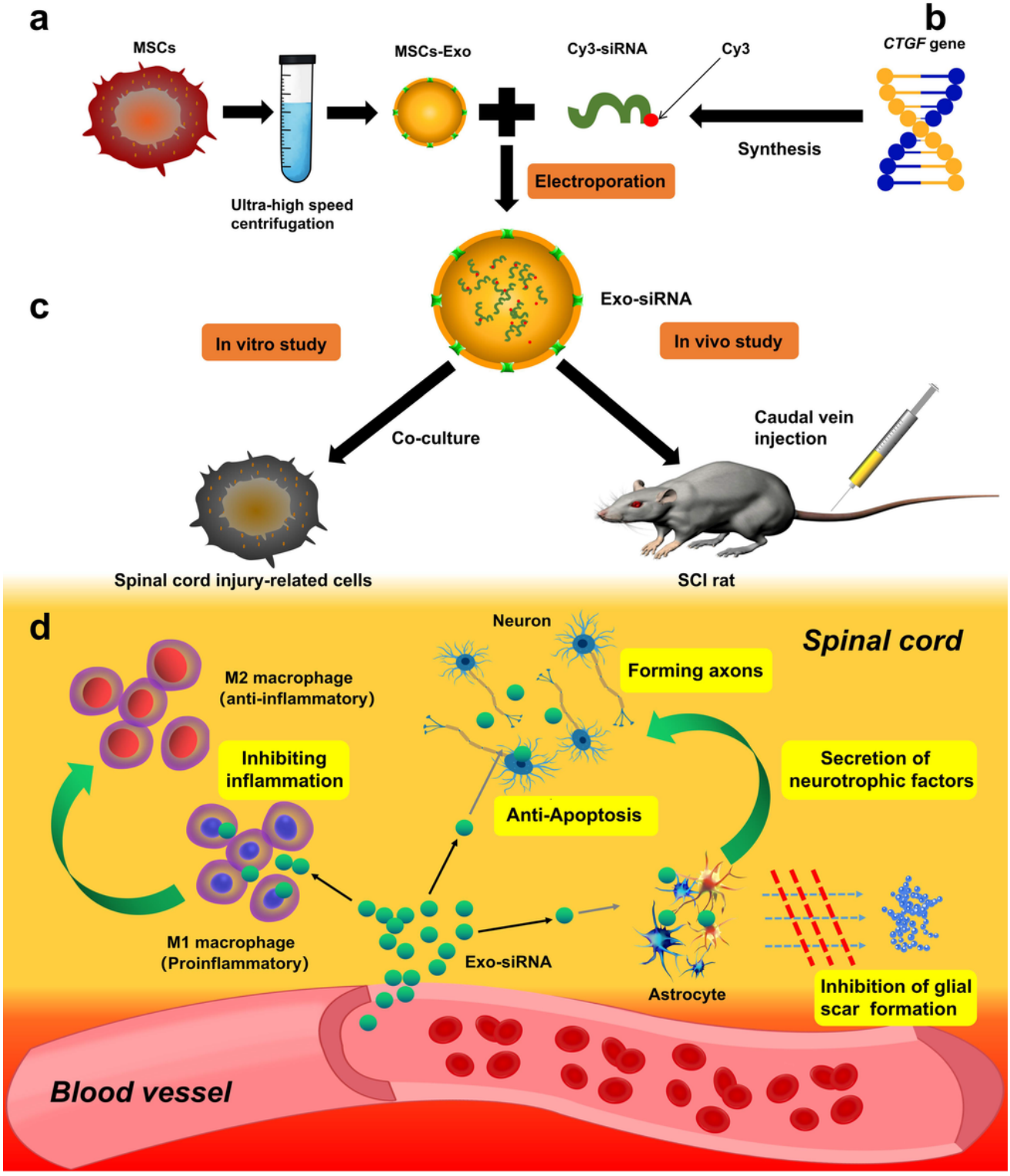


Figure 1

Schematic illustration of the experimental procedure. (a) Exo were extracted from MSCs by ultrahigh-speed centrifugation. (b) Meanwhile, siRNA with silencing effect was designed and synthesized according to the sequences of the rat Ctgf gene. (c) Then siRNA was loaded into Exo by electroporation to construct Exo-siRNA. Finally, the obtained Exo-siRNA was co-cultured with cells in various SCI

environments and administered to SCI rats by tail vein injection. (d) The therapeutic effects of Exo-siRNA on macrophages, astrocytes and neurons of the impaired spinal cord segments were determined.

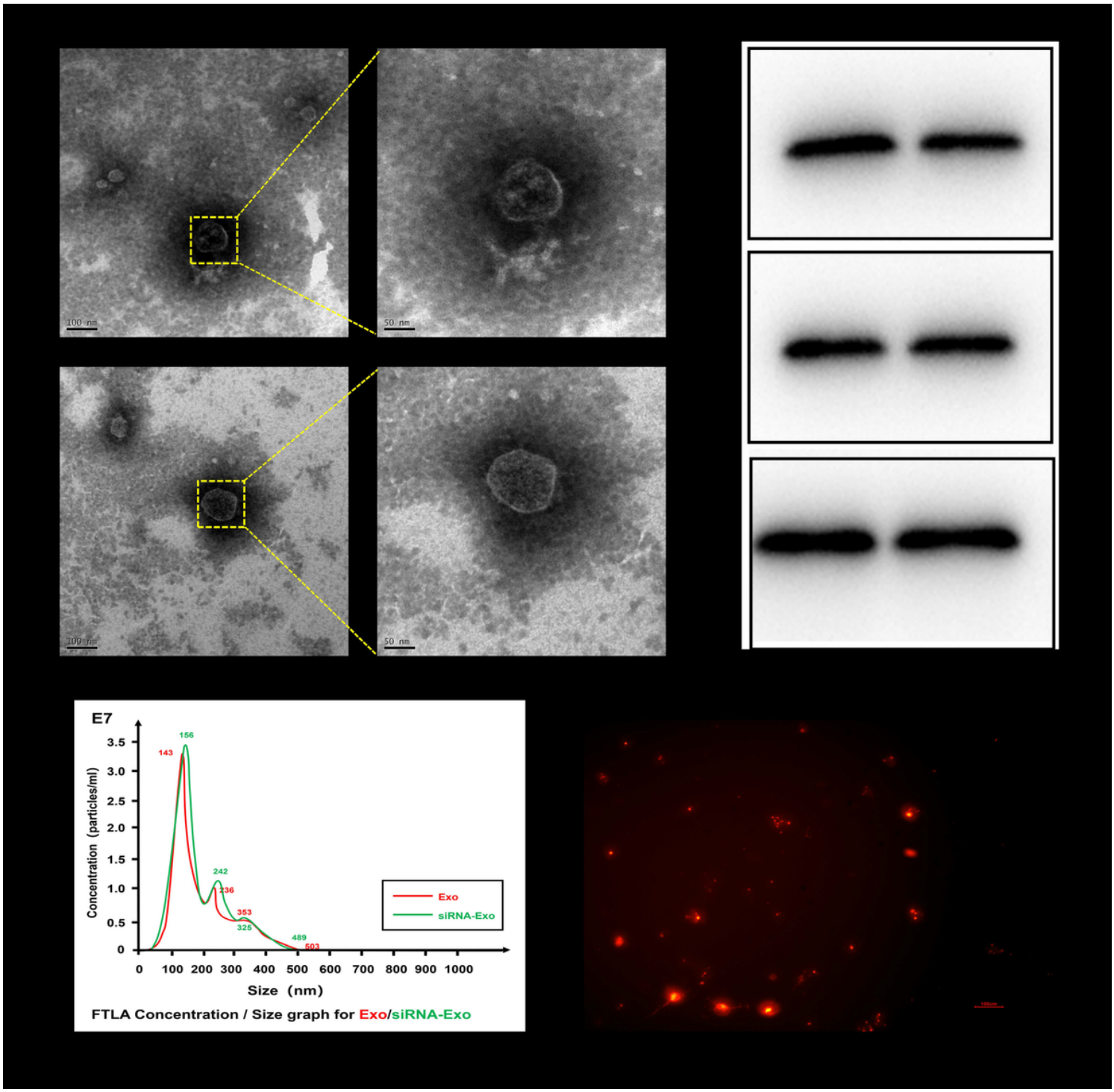


Figure 2

Characterization of Exo and Exo-siRNA. (a) TEM revealed the typical exosome structure of Exo and Exo-siRNA. (b) NTA analysis of Exo and Exo-siRNA showed the incorporation of siRNA did not affect the diameter of Exo. (c) The exosome marker proteins, CD9 and CD63, were analyzed by WB. (d) Exo stained by fluorescence of DiIC18 amethylindocarbocyanine were exhibited, scale bar =100 μm.

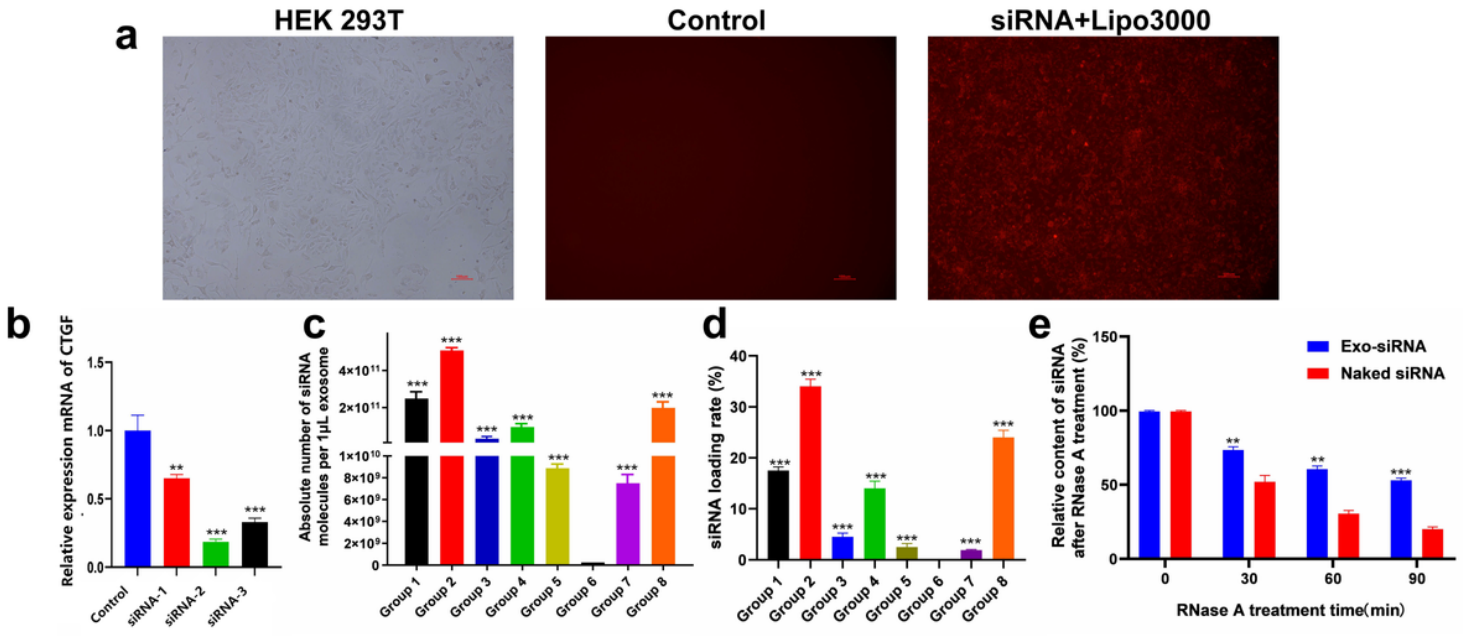


Figure 3

Preliminarily analysis of silencing efficiency of three pairs of target siRNA. (a) Cy3-siRNA was transfected into HEK293T cells by Lipo3000, and the control group was not transfected. (b) The expressions of Ctgf-related mRNAs at 72 h after siRNA transfection were presented. n = 3, *p < 0.05, **p < 0.01 v.s. Control. (c) The absolute number of siRNA molecules in Exo under different electroporation conditions was exhibited. n = 3, *p < 0.05, **p < 0.01 v.s. Group 6. (d) The loading rates of siRNA in Exo under different electroporation conditions were presented. n = 3, *p < 0.05, **p < 0.01 v.s. Group 6. (e) Relative contents of naked siRNA and Exo-siRNA after RNase treatment were showed. n = 3, *p < 0.05, **p < 0.01 v.s. naked siRNA.

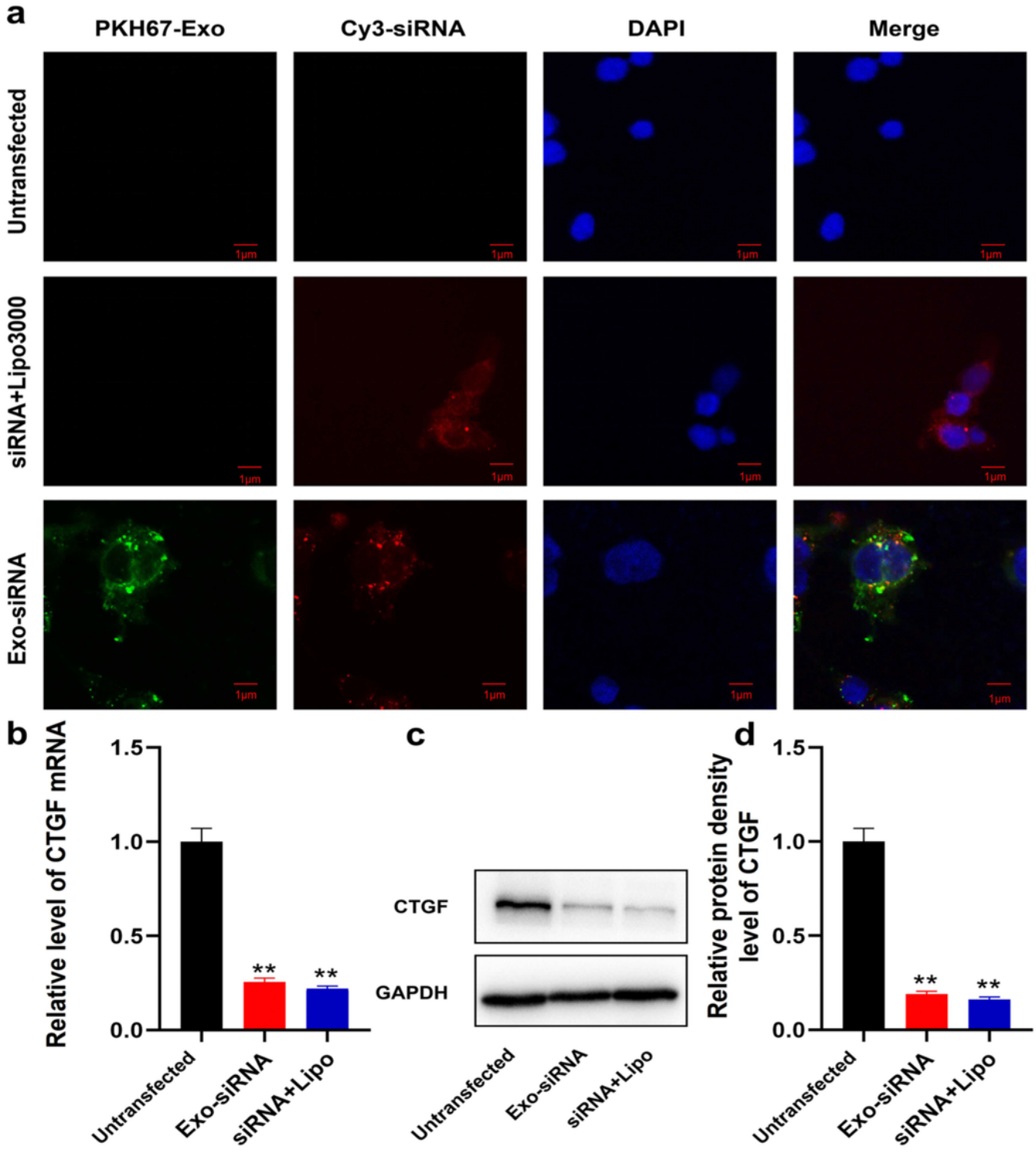


Figure 4

Exo-siRNA could effectively inhibit the expression of Ctgf gene in astrocytes and up-regulate the secretion of neurotrophic factors and anti-inflammatory factors in the impaired spinal cord segments. (a) Fluorescence patterns of LPS/hypoxia-treated astrocytes after co-culture with PKH67 and Cy3 double-labeled Exo-siRNA for 72 h were assessed. (b) The relative expression of Ctgf mRNA after Exo-siRNA co-culture for 72 h was determined, n = 3, *p < 0.05, **p < 0.01 v.s. Control. (c) The expressions of CTGF-

related proteins, BDNF (a neurotrophic factor) and TGF-β1 (an anti-inflammatory factor) at 72 h after Exo-siRNA treatment were detected. n = 3, *p < 0.05, **p < 0.01 v.s. Control.

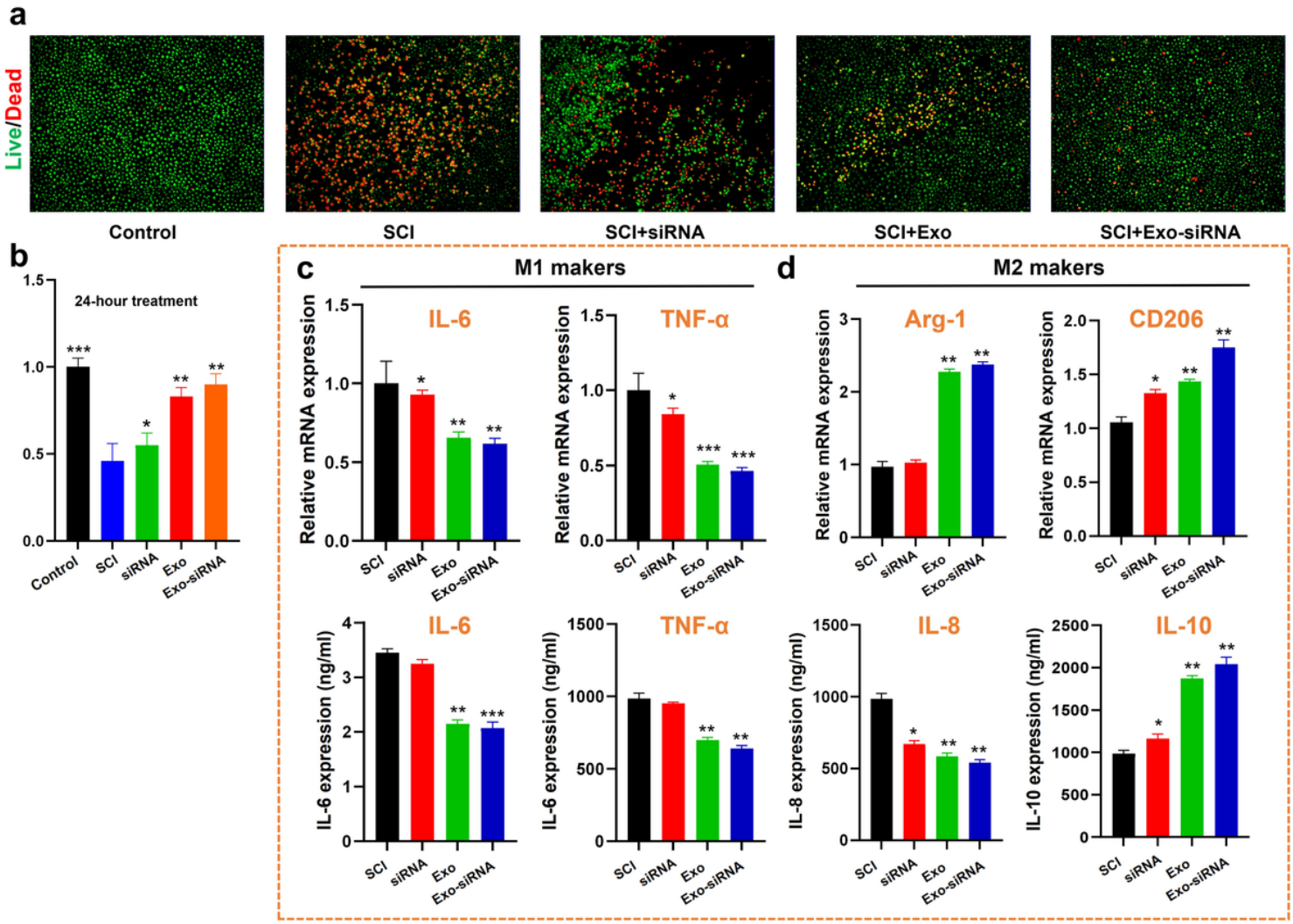


Figure 5

Ameliorative effects of Exo-siRNA on DRGs and macrophages in SCI environment in vitro. (a-b) Anti-apoptotic effect of siRNA-Exo on DRGs was assessed. (a) Living and death staining patterns of LPS/hypoxia-treated DRGs were analyzed at 24 h after co-culture with Exo-siRNA, siRNA, Exo and PBS respectively. Living and dead cells were stained with calcein-AM (green) and propidium iodide (red), while the control group did not receive any treatment. scale bar =100 μm. (b) Cell survival rate of LPS/hypoxia-treated DRGs was calculated by CCK-8 at 24 h after co-culture with Exo-siRNA, siRNA, Exo and PBS. n = 3, *p < 0.05, **p < 0.01 v.s. LPS/hypoxia. (c-d) qRT-PCR analysis was performed for mRNA expressions and ELISA analysis for secretion of (c) M1-related pro-inflammatory cytokines and (d) markers of M2 macrophage phenotypes in LPS/hypoxia-treated NR8383 macrophages at 48 h after siRNA-Exo, siRNA, Exo and PBS administrations. n = 3, *p < 0.05, **p < 0.01 v.s. LPS/hypoxia.

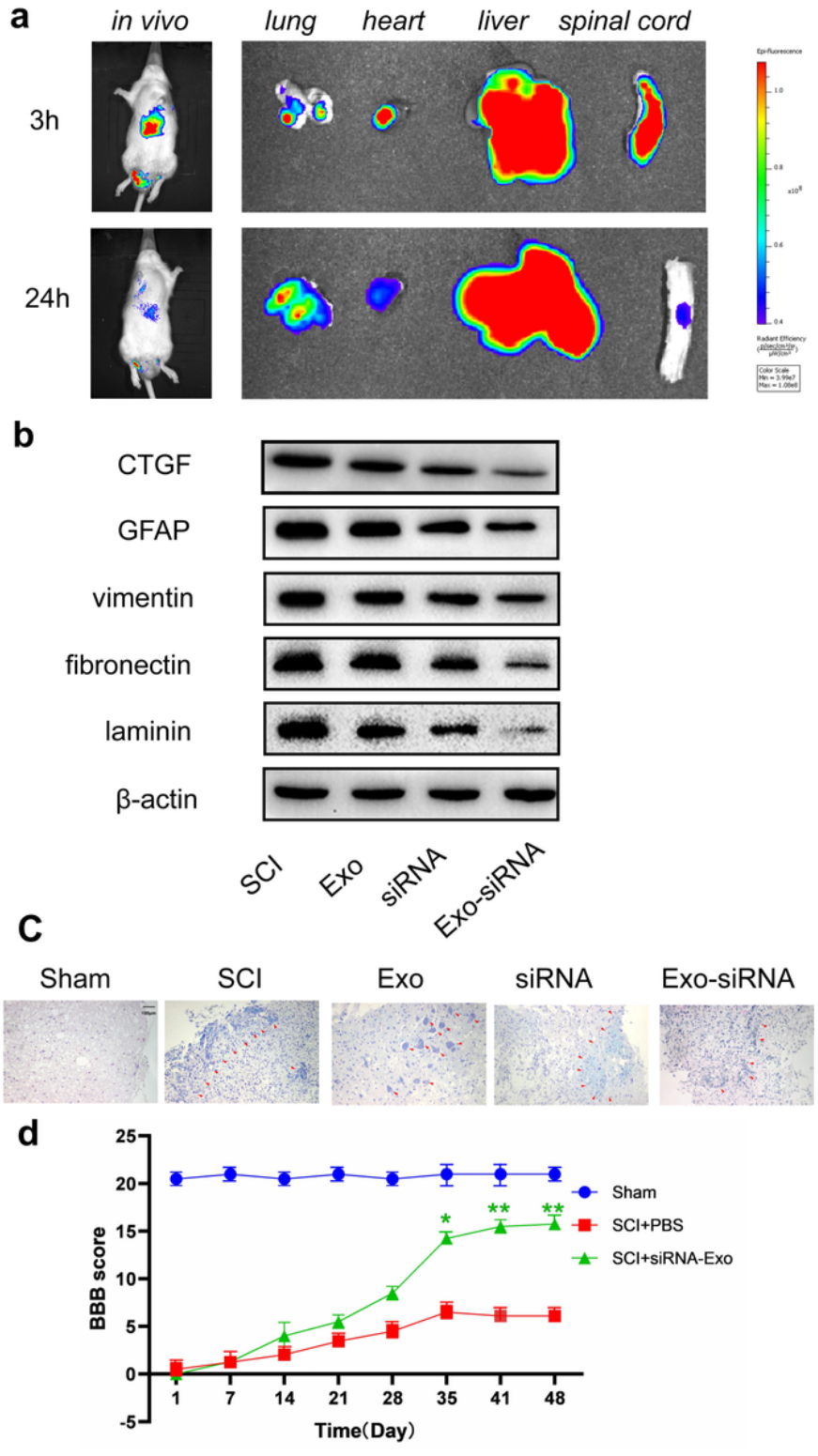


Figure 6

Therapeutic effects of Exo-siRNA on SCI rats. Rats were classified into SCI group, Sham group, Exo group and Exo-siRNA group, n = 6. (a) Fluorescence imaging of organs of Exo-siRNA group at 3 h, 24 h and 48 h after intravenous injection was illustrated. (b) Expressions of GFAP, vimentin, fibronectin and laminin were assessed by WB, *p < 0.05, **p < 0.01 v.s. SCI group. (c) Transverse sections of core lesion tissues in each group were stained by Masson's trichrome method. Fibrotic tissue area was indicated by red arrows. Bars

= 100 μm. (d) Recovery of motor dysfunction of rats in SCI group, Sham group, Exo group and Exo-siRNA group was analyzed by BBB score. n = 6, *p < 0.05, **p < 0.01 v.s. SCI group.

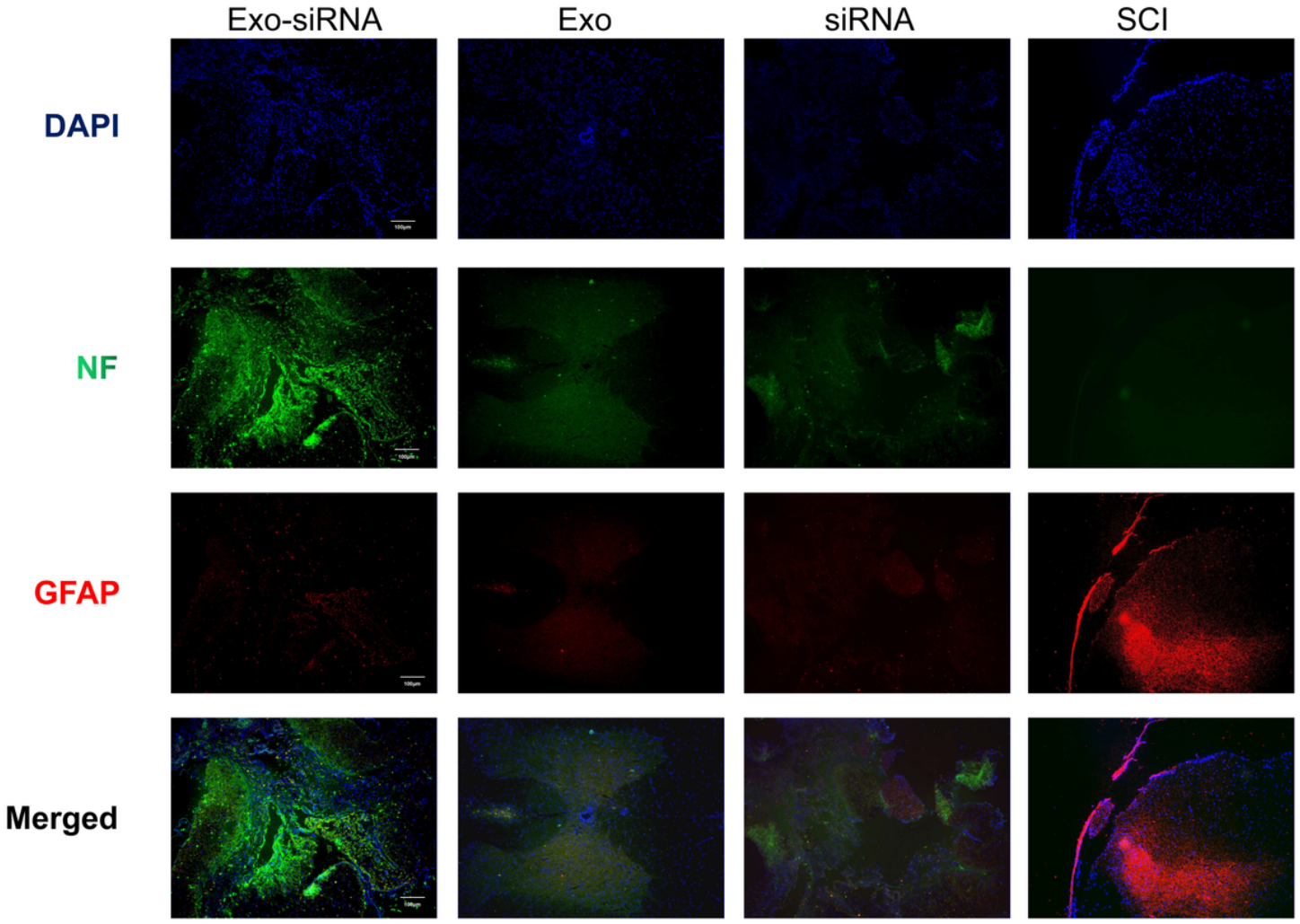


Figure 7

Expressions and distribution of neuron (NF, green) and astrogliosis (GFAP, red) in longitudinal sections of the injured spinal cord segments at 28 days after injury were assessed by immunofluorescence analysis. Bars = 100 μm.